Josephson current and Andreev states in superconductor–half metal–superconductor heterostructures

Artem V. Galaktionov and Mikhail S. Kalenkov
I.E. Tamm Department of Theoretical Physics, P.N. Lebedev Physics Institute, 119991 Moscow, Russia

Andrei D. Zaikin
Forschungszentrum Karlsruhe, Institut für Nanotechnologie, 76021, Karlsruhe, Germany
and I.E. Tamm Department of Theoretical Physics, P.N. Lebedev Physics Institute, 119991 Moscow, Russia
(Received 30 November 2007; published 28 March 2008)

We develop a detailed microscopic theory describing dc Josephson effect and Andreev bound states in superconducting junctions with a half metal. In such systems, the supercurrent is caused by triplet pairing states emerging due to spin-flip scattering at the interfaces between superconducting electrodes and the half metal. For sufficiently clean metals, we provide a detailed nonperturbative description of the Josephson current at arbitrary transmissions and spin-flip scattering parameters for both interfaces. Our analysis demonstrates that the behavior of both the Josephson current and Andreev bound states crucially depends on the strength of spin-flip scattering, showing a rich variety of features which can be tested in future experiments.

DOI: 10.1103/PhysRevB.77.094520 PACS number(s): 74.50.+r, 73.40.−c, 74.45.+c

I. INTRODUCTION

Recent experiments[1] strongly indicate the possibility to realize nonvanishing supercurrent across sufficiently thick half-metal (H) layers embedded in between two *s*-wave BCS superconductors (S). This physical situation appears rather nontrivial. Indeed, in conventional SNS junctions (N stands for spin-isotropic normal metal), the supercurrent is carried by (spin-singlet) Cooper pairs penetrating into the N-metal layer from both superconductors due to the proximity effect. However, half metals are fully spin polarized materials acting as insulators for electrons with one of the two spin directions. Hence, penetration of spin-singlet electron pairs into half metals should be prohibited, and no supercurrent would be possible.

Recently, it was realized[2] that this situation changes qualitatively if one allows for spin-flip scattering at HS interfaces. Such scattering enables conversion of spin-singlet pairing in S electrodes into spin-triplet pairing in a half metal. In this way, superconducting correlations can survive even in a half-metal ferromagnet, thus "unblocking" the supercurrent across SHS junctions. Subsequent numerical and analytical studies[3–5] confirmed this physical picture also extending it to structures with disorder. In particular, it was argued[5] that depending on the degree of disorder in the H metal, the origin of triplet pairing there can change from the *p*-wave type to the odd-frequency one.[6] It was also realized that the presence of triplet pairing in strong ferromagnets and in half metals can cause the so-called π-junction behavior of the system.[7]

Despite all these important developments, the issue is yet far from settled. The goal of this paper is to work out a complete theory of dc Josephson effect in clean SHS heterostructures at arbitrary transmissions of HS interfaces. Electron scattering at these interfaces will be described by the most general scattering matrices which fully account for spin-flip processes. Depending on the system parameters, we will find a rich variety of the results both for the temperature dependence of the supercurrent and for the current-phase relation in SHS junctions, demonstrating crucial importance of spin-flip scattering at HS interfaces. In addition, we will also address Andreev level quantization and show that this phenomenon in SHS junctions acquires features which are not present in conventional SNS structures.

The structure of the paper is as follows. In Sec. II, we will employ the quasiclassical formalism which enables us to exactly evaluate the Josephson current in SHS structures with many conducting channels at any transmissions of SH interfaces. In Sec. III, we will develop a more general approach which also accounts for resonant effects and allows us to include structures with few conducting channels into consideration. Within this approach, we will describe both the Josephson current and Andreev levels in SHS junctions and establish the correspondence to the results derived in Sec. II. In Sec. IV, we will briefly summarize our main observations.

II. QUASICLASSICAL ANALYSIS

In this section, we will consider a general model of a clean SNS junction with spin-active interfaces. We will then specify the scattering matrices of NS interfaces in a way appropriate to describe SHS heterostructures. Here, we will treat the systems with many conducting channels. For this reason, it will be sufficient to employ the quasiclassical formalism of energy-integrated Matsubara Green's functions.[8,9]

A. Riccati parametrization

In the ballistic limit, the Eilenberger equations take the form

$$[i\omega_n\hat{\tau}_3 - \hat{\Delta}(\boldsymbol{r}), \hat{g}(\boldsymbol{p}_F, \omega_n, \boldsymbol{r})] + i\boldsymbol{v}_F \nabla \hat{g}(\boldsymbol{p}_F, \omega_n, \boldsymbol{r}) = 0, \quad (1)$$

where $[\hat{a}, \hat{b}] = \hat{a}\hat{b} - \hat{b}\hat{a}$, $\omega_n = \pi T(2n+1)$ is Matsubara frequency, $\boldsymbol{p}_F = m\boldsymbol{v}_F$ is the electron Fermi momentum vector, and $\hat{\tau}_3$ is the Pauli matrix in Nambu space. The function $\hat{g}$

also obeys the normalization condition $\hat{g}^2=1$. Green's function $\hat{g}$ and $\hat{\Delta}$ are 4×4 matrices in Nambu and spin spaces. In Nambu space, they can be parametrized as

$$\hat{g}=\begin{pmatrix} g & f \\ \tilde{f} & \tilde{g} \end{pmatrix}, \quad \hat{\Delta}=\begin{pmatrix} 0 & \Delta i\sigma_2 \\ \Delta^* i\sigma_2 & 0 \end{pmatrix}, \tag{2}$$

where g, f, $\tilde{f}$, and $\tilde{g}$ are 2×2 matrices in the spin space, Δ is the BCS order parameter, and σ_i are Pauli matrices. For simplicity, we will only consider the case of spin-singlet isotropic pairing in superconducting electrodes. As usual, the superconducting order parameter in the normal layer is set to be equal to zero.

The equilibrium current density is defined by the standard relation

$$\boldsymbol{j}(\boldsymbol{r})=eN_0\pi T\sum_{\omega_n>0}\mathrm{Im}\langle \boldsymbol{v}_F\,\mathrm{Sp}[\hat{\tau}_3\hat{g}(\boldsymbol{p}_F,\omega_n,\boldsymbol{r})]\rangle, \tag{3}$$

where $N_0=mp_F/2\pi^2$ is the density of states at the Fermi level and angular brackets $\langle\cdots\rangle$ denote averaging over the Fermi momentum.

The above matrix Green's functions can be conveniently parametrized[10] by the two Riccati amplitudes γ and $\tilde{\gamma}$:

$$\hat{g}=\begin{pmatrix} (1-\gamma\tilde{\gamma})^{-1}(1+\gamma\tilde{\gamma}) & 2(1-\gamma\tilde{\gamma})^{-1}\gamma \\ -2(1-\tilde{\gamma}\gamma)^{-1}\tilde{\gamma} & -(1-\tilde{\gamma}\gamma)^{-1}(1+\tilde{\gamma}\gamma) \end{pmatrix}. \tag{4}$$

With the aid of the above parametrization, one can identically transform the quasiclassical equations (1) into the following set of decoupled equations for Riccati amplitudes:[10]

$$i\boldsymbol{v}_F\nabla\gamma+2i\omega\gamma=\gamma\Delta^* i\sigma_2\gamma-\Delta i\sigma_2, \tag{5}$$

$$i\boldsymbol{v}_F\nabla\tilde{\gamma}-2i\omega\tilde{\gamma}=\tilde{\gamma}\Delta i\sigma_2\tilde{\gamma}-\Delta^* i\sigma_2. \tag{6}$$

Solving Eqs. (5) and (6) inside the normal metal, we obtain the following relations between Riccati amplitudes:

$$\gamma_+=\Gamma_{1'}\exp(-\omega_n d/|v_{Fx}|)=\gamma_{2'}\exp(\omega_n d/|v_{Fx}|), \tag{7}$$

$$\gamma_-=\gamma_{1'}\exp(\omega_n d/|v_{Fx}|)=\Gamma_{2'}\exp(-\omega_n d/|v_{Fx}|), \tag{8}$$

$$\tilde{\gamma}_+=\tilde{\gamma}_{1'}\exp(\omega_n d/|v_{Fx}|)=\tilde{\Gamma}_{2'}\exp(-\omega_n d/|v_{Fx}|), \tag{9}$$

$$\tilde{\gamma}_-=\tilde{\Gamma}_{1'}\exp(-\omega_n d/|v_{Fx}|)=\tilde{\gamma}_{2'}\exp(\omega_n d/|v_{Fx}|), \tag{10}$$

where $\gamma_{i'}$, $\Gamma_{i'}$, $\tilde{\gamma}_{i'}$, and $\tilde{\Gamma}_{i'}$ are Riccati amplitudes at the corresponding interface, $\gamma_\pm$ and $\tilde{\gamma}_\pm$ are Riccati amplitudes in the middle of the normal metal slab (see Fig. 1 for details), and d is a distance between two NS interfaces.

Deep inside the superconducting electrodes, we apply the following asymptotic conditions:

$$\gamma_1=-\sigma_2 a(\omega)e^{-i\chi/2}, \quad \tilde{\gamma}_1=\sigma_2 a(\omega)e^{i\chi/2}, \tag{11}$$

$$\gamma_2=-\sigma_2 a(\omega)e^{i\chi/2}, \quad \tilde{\gamma}_2=\sigma_2 a(\omega)e^{-i\chi/2}, \tag{12}$$

where $a(\omega)=(\sqrt{\omega^2+|\Delta|^2}-\omega)/|\Delta|$ and χ is the superconducting phase difference across the junction. Here and below, we assume that the order parameter is spatially uniform inside superconducting electrodes. This choice can always be parametrically justified by assuming the proper junction geometry and/or interface transmission values. For simplicity, we also assume that the absolute values of the superconducting order parameter are identical in both S electrodes. A generalization of our approach to the case of anisotropic pairing and asymmetric electrodes with $|\Delta_1|\neq|\Delta_2|$ is straightforward.

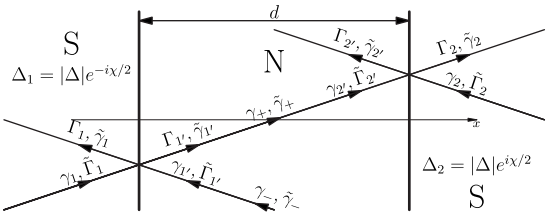

FIG. 1. SNS junction and Riccati amplitudes in the clean limit. The functions γ_i, Γ_i and $\tilde{\gamma}_i$, $\tilde{\Gamma}_i$ are Riccati amplitudes at the corresponding NS interface. $\gamma_\pm$ and $\tilde{\gamma}_\pm$ are Riccati amplitudes in the middle of the normal metal layer. Quasiparticle momentum directions are indicated by arrows.

B. Boundary conditions at metallic interfaces

The above quasiclassical equations should be supplemented by appropriate boundary conditions at the interfaces. In the case of specularly reflecting spin-degenerate interfaces, these conditions were derived by Zaitsev[11] and later generalized to spin-active interfaces in Ref. 12.

Similarly to Ref. 13, it will be convenient for us to use the boundary conditions formulated directly in terms of Riccati amplitudes. Let us consider the first NS interface and explicitly specify the relations between Riccati amplitudes for incoming and outgoing electron trajectories, see Fig. 1. For instance, the boundary conditions for Γ_1 can be written in the form[14,15]

$$\Gamma_1=r_{1l}\gamma_1\underline{S}^+_{11}+t_{1l}\gamma_{1'}\underline{S}^+_{11'}, \tag{13}$$

$$\tilde{\Gamma}_1=\underline{S}^+_{11}\tilde{\gamma}_1\tilde{r}_{1r}+\underline{S}^+_{1'1}\tilde{\gamma}_{1'}\tilde{t}_{1r}. \tag{14}$$

Here, we defined the transmission (t) and reflection (r) amplitudes as

$$r_{1l}=[\beta^{-1}_{1'1}S^+_{11}-\beta^{-1}_{1'1'}S^+_{11'}]^{-1}\beta^{-1}_{1'1}, \tag{15}$$

$$\tilde{r}_{1r}=\beta^{-1}_{11'}[S^+_{11}\beta^{-1}_{11'}-S^+_{1'1}\beta^{-1}_{1'1'}]^{-1}, \tag{16}$$

$$t_{1l}=-[\beta^{-1}_{1'1}S^+_{11}-\beta^{-1}_{1'1'}S^+_{11'}]^{-1}\beta^{-1}_{1'1'}, \tag{17}$$

$$\tilde{t}_{1r}=-\beta^{-1}_{1'1'}[S^+_{11}\beta^{-1}_{11'}-S^+_{1'1}\beta^{-1}_{1'1'}]^{-1}, \tag{18}$$

where

$$\beta_{ij}=S^+_{ij}-\gamma_j\underline{S}^+_{ij}\tilde{\gamma}_i. \tag{19}$$

Matrices S_{ij} and $\underline{S}_{ij}$ are the building blocks of the full electron and hole interface S matrices,[12]

$$\mathcal{S}=\begin{pmatrix} S_{11} & S_{11'} \\ S_{1'1} & S_{1'1'} \end{pmatrix}, \quad \underline{\mathcal{S}}=\begin{pmatrix} \underline{S}_{11} & \underline{S}_{11'} \\ \underline{S}_{1'1} & \underline{S}_{1'1'} \end{pmatrix}. \tag{20}$$

Boundary conditions for $\Gamma_{1'}$, $\tilde{\Gamma}_{1'}$ can be obtained from the above equations simply by replacing $1 \leftrightarrow 1'$. Boundary conditions describing electron scattering at the second interface are formulated analogously.

Combining the above relations between Riccati amplitudes, we obtain matrix quadratic equations for the matrices $\eta_\pm = -i\gamma_\pm\sigma_2$ and $\tilde{\eta}_\pm = i\sigma_2\tilde{\gamma}_\pm$,

$$\begin{aligned} &\eta_+\{c_2a_1\exp(-\omega_n d/|v_{Fx}|)+a_2b_1\exp(\omega_n d/|v_{Fx}|)\}\eta_+ \\ &\quad -\eta_+\{c_2c_1\exp(-2\omega_n d/|v_{Fx}|)+a_2d_1\}+\{d_2a_1 \\ &\quad +b_2b_1\exp(2\omega_n d/|v_{Fx}|)\}\eta_+ -\{d_2c_1\exp(-\omega_n d/|v_{Fx}|) \\ &\quad +b_2d_1\exp(\omega_n d/|v_{Fx}|)\}=0, \end{aligned} \tag{21}$$

$$\begin{aligned} &\tilde{\eta}_+\{d_2c_1\exp(-\omega_n d/|v_{Fx}|)+b_2d_1\exp(\omega_n d/|v_{Fx}|)\}\tilde{\eta}_+ -\tilde{\eta}_+\{d_2a_1 \\ &\quad +b_2b_1\exp(2\omega_n d/|v_{Fx}|)\}+\{c_2c_1\exp(-2\omega_n d/|v_{Fx}|) \\ &\quad +a_2d_1\}\tilde{\eta}_+ -\{c_2a_1\exp(-\omega_n d/|v_{Fx}|) \\ &\quad +a_2b_1\exp(\omega_n d/|v_{Fx}|)\}=0, \end{aligned} \tag{22}$$

where we introduced the following 2×2 matrices:

$$a_1=[i\sigma_2\underline{S}^+_{11'}\tilde{\gamma}_1\beta^{-1}_{11}S^+_{1'1}], \tag{23}$$

$$b_1=[S^+_{1'1'}-S^+_{11'}\beta^{-1}_{11}S^+_{1'1}], \tag{24}$$

$$c_1=[\sigma_2(\underline{S}^+_{1'1'}+\underline{S}^+_{11'}\tilde{\gamma}_1\beta^{-1}_{11}\gamma_1\underline{S}^+_{1'1})\sigma_2], \tag{25}$$

$$d_1=[S^+_{11'}\beta^{-1}_{11}\gamma_1\underline{S}^+_{1'1}i\sigma_2], \tag{26}$$

$$a_2=[i\sigma_2\underline{S}^+_{22'}\tilde{\gamma}_2\beta^{-1}_{22}S^+_{2'2}], \tag{27}$$

$$b_2=[S^+_{2'2'}-S^+_{22'}\beta^{-1}_{22}S^+_{2'2}], \tag{28}$$

$$c_2=[\sigma_2(\underline{S}^+_{2'2'}+\underline{S}^+_{22'}\tilde{\gamma}_2\beta^{-1}_{22}\gamma_2\underline{S}^+_{2'2})\sigma_2], \tag{29}$$

$$d_2=[S^+_{22'}\beta^{-1}_{22}\gamma_2\underline{S}^+_{2'2}i\sigma_2]. \tag{30}$$

Matrix equations for the η_- and $\tilde{\eta}_-$ can be obtained from Eqs. (21) and (22) by substituting $\eta_+ \to \eta_-$, $\tilde{\eta}_+ \to \tilde{\eta}_-$ and interchanging of indices $1 \leftrightarrow 2$.

For arbitrary interface S matrices, the matrix equations (21) and (22) can be reduced to scalar quartic equations with very cumbersome general solutions. These solutions, however, become simpler for some particular interface models. Here, we will stick to the case of SHS junctions in which we should specify the scattering S matrix for the interface between spin-isotropic normal metal (or superconductor) and fully spin polarized ferromagnet. We will demonstrate that in this case, Eqs. (21) and (22) can be solved in a transparent and compact way.

C. Scattering matrices

Let us specify the scattering S matrices for both SH interfaces. For simplicity, we will assume that these matrices depend only on the incidence angle but not on the azimuthal one. Then, the following relation between electron and hole S matrices holds: $\mathcal{S}=\underline{\mathcal{S}}^T$. For a half-metal slab between two superconducting electrodes, the corresponding interface scattering matrices contain 3×3 nontrivial submatrices, i.e.,

$$\mathcal{S}=\begin{pmatrix} \cdots & \cdots & \cdots & 0 \\ \cdots & \cdots & \cdots & 0 \\ \cdots & \cdots & \cdots & 0 \\ 0 & 0 & 0 & 1 \end{pmatrix}. \tag{31}$$

It is straightforward to demonstrate that the Josephson current is invariant under the following transformation of the S matrices:

$$\mathcal{S}_1 \to \begin{pmatrix} U_1 & 0 \\ 0 & V \end{pmatrix}\mathcal{S}_1\begin{pmatrix} U_1^+ & 0 \\ 0 & V^+ \end{pmatrix}, \tag{32}$$

$$\underline{\mathcal{S}}_1 \to \begin{pmatrix} U_1^* & 0 \\ 0 & V^* \end{pmatrix}\underline{\mathcal{S}}_1\begin{pmatrix} U_1^T & 0 \\ 0 & V^T \end{pmatrix}, \tag{33}$$

$$\mathcal{S}_2 \to \begin{pmatrix} U_2 & 0 \\ 0 & V \end{pmatrix}\mathcal{S}_2\begin{pmatrix} U_2^+ & 0 \\ 0 & V^+ \end{pmatrix}, \tag{34}$$

$$\underline{\mathcal{S}}_2 \to \begin{pmatrix} U_2^* & 0 \\ 0 & V^* \end{pmatrix}\underline{\mathcal{S}}_2\begin{pmatrix} U_2^T & 0 \\ 0 & V^T \end{pmatrix}, \tag{35}$$

where $U_1, U_2, V \in \mathrm{SU}(2)$. With the aid of the above transformation, we can always reduce the S matrices to the following form:

$$\mathcal{S}=\begin{pmatrix} \alpha e^{i\zeta}\cos\nu & \beta e^{i\zeta} & \alpha e^{-2i\zeta}\sin\nu & 0 \\ -\beta^* e^{i\zeta}\cos\nu & \alpha^* e^{i\zeta} & -\beta^* e^{-2i\zeta}\sin\nu & 0 \\ -e^{i\zeta}\sin\nu & 0 & e^{-2i\zeta}\cos\nu & 0 \\ 0 & 0 & 0 & 1 \end{pmatrix}, \tag{36}$$

where $|\alpha|^2+|\beta|^2=1$ and ν, ζ are real. We also note that, in general, the first and the second interfaces are characterized by two different sets of parameters α, β, ν and ζ, i.e., these interfaces are described by different scattering matrices.

Here and below, the parameter $\sin^2\nu$ defines an effective interface transmission. The normal state differential conductance (dI/dV) for the metallic interface described by the $\mathcal{S}$ matrix (36) is proportional to $\sin^2\nu$,

$$G_{NN}=\frac{\mathcal{A}e^2}{2\pi}\int_{|p_\parallel|<p_F}\frac{d^2p_\parallel}{(2\pi)^2}\sin^2\nu=\frac{e^2}{2\pi}\sum_k \sin^2\nu, \tag{37}$$

where the index k labels conducting channels of our junction. The limit $\nu=0$ corresponds to completely impenetrable interfaces. The parameter β is responsible for spin-flip scattering of electrons at the interface.

Finally, we point out that by virtue of Eqs. (32), (33), and (35), the scattering matrix employed in the analysis of Ref. 4 can be reduced to our expression (36) provided we identify

$$\cos\nu = 1 - \frac{t_{\uparrow\uparrow}^2 + t_{\downarrow\uparrow}^2}{2W}, \quad \sin\nu = \frac{\sqrt{t_{\uparrow\uparrow}^2 + t_{\downarrow\uparrow}^2}}{W}, \tag{38}$$

$$\alpha = -\frac{t_{\uparrow\uparrow}^2}{t_{\uparrow\uparrow}^2 + t_{\downarrow\uparrow}^2} e^{i\theta/2} - \frac{t_{\downarrow\uparrow}^2}{t_{\downarrow\uparrow}^2 + t_{\downarrow\uparrow}^2} e^{-i\theta/2}, \tag{39}$$

$$\beta = 2i\frac{t_{\uparrow\uparrow} t_{\downarrow\uparrow}}{t_{\uparrow\uparrow}^2 + t_{\downarrow\uparrow}^2} \sin\left(\frac{\theta}{2}\right) e^{-i(\theta_{\uparrow\uparrow} + \theta_{\downarrow\uparrow})}, \quad \zeta = 0, \tag{40}$$

where we use the notations from Ref. 4.

D. Josephson current

Now, we are ready to evaluate the Josephson current. In SNS systems with interface S matrices of the form (36), the matrices a_i, b_i, c_i, d_i, $\eta_\pm$, and $\tilde{\eta}_\pm$ have the following structure:

$$a_i = \begin{pmatrix} 0 & 0 \\ a_i & 0 \end{pmatrix}, \quad b_i = \begin{pmatrix} b_i & 0 \\ 0 & 1 \end{pmatrix}, \quad c_i = \begin{pmatrix} 1 & 0 \\ 0 & c_i \end{pmatrix}, \tag{41}$$

$$d_i = \begin{pmatrix} 0 & d_i \\ 0 & 0 \end{pmatrix}, \quad \eta_\pm = \begin{pmatrix} 0 & \eta_\pm \\ 0 & 0 \end{pmatrix}, \quad \tilde{\eta}_\pm = \begin{pmatrix} 0 & 0 \\ \tilde{\eta}_\pm & 0 \end{pmatrix}. \tag{42}$$

Since all the matrices a_i, b_i, c_i, d_i, $\eta_\pm$, and $\tilde{\eta}_\pm$ have only one nontrivial matrix element, it suffices to denote this element by the same symbol as the corresponding matrix itself. Then, from Eqs. (21) and (22), we derive a simple quadratic equations for the scalar variables $\eta_\pm$ and $\tilde{\eta}_\pm$. Resolving this equation and making use of the Riccati parametrization described in Secs. II A and II B, we construct the Green-Eilenberger function for our junction. Substituting this function into Eq. (3), we arrive at the following general result for the Josephson current:

$$I(\chi) = -4e\mathcal{A}T \sum_{\omega_n > 0} \int_{|p_\parallel| < p_F} \frac{d^2 p_\parallel}{(2\pi)^2} \frac{a^2(1-a^2)^2 \mathcal{D}_{12} \sin\tilde{\chi}}{Q(\omega_n)}, \tag{43}$$

where $\mathcal{D}_{12} = |\beta_1||\beta_2| \sin^2\nu_1 \sin^2\nu_2$, $\mathcal{A}$ is the junction cross section,

$$\begin{aligned} Q(\omega) = \Bigg\{ \Bigg[& 2a^2(1-a^2)^2 |\beta_1||\beta_2| \sin^2\nu_1 \sin^2\nu_2 \cos\tilde{\chi} - [(1-a^2) \\ & \times (1 - a^2\cos^2\nu_1) + a^2|\tilde{\alpha}_1|^2][(1-a^2)(1-a^2\cos^2\nu_2) \\ & + a^2|\tilde{\alpha}_2|^2] \exp\left(\frac{2\omega_n d}{|v_{Fx}|}\right) - [(1-a^2)(-a^2 + \cos^2\nu_1) \\ & + a^2|\tilde{\alpha}_1|^2][(1-a^2)(-a^2 + \cos^2\nu_2) \\ & + a^2|\tilde{\alpha}_2|^2] \exp\left(\frac{-2\omega_n d}{|v_{Fx}|}\right) \Bigg]^2 - 4|(1-a^2)^2 \cos\nu_1 \\ & + a^2\tilde{\alpha}_1^2|^2 (1-a^2)^2 \cos\nu_2 + a^2\tilde{\alpha}_2^2|^2 \Bigg\}^{1/2}, \end{aligned} \tag{44}$$

and

$$\tilde{\chi} = \chi + 3\zeta_2 + \arg\beta_2 - 3\zeta_1 - \arg\beta_1, \quad \tilde{\alpha}_i = \alpha_i + \alpha_i^* \cos\nu_i. \tag{45}$$

We observe that the Josephson current is proportional to the parameter $\mathcal{D}_{12}$ which contains effective transmissions of both interfaces $\sin^2\nu_1 \sin^2\nu_2$ and the two spin-flip factors $|\beta_1|$ and $|\beta_2|$. The scattering matrix parameters ζ_1, $\arg\beta_1$, ζ_2, and $\arg\beta_2$ enter into our result only in combination with the phase difference χ [Eq. (45)].

Let us briefly analyze the above general expression for the Josephson current. At small transmissions $\nu_1, \nu_2 \ll 1$ and for sufficiently long junctions $d \gg \xi_0(\nu_1^2 + \nu_2^2)$, Eq. (43) reduces to

$$\begin{aligned} I(\chi) = & -\frac{e\mathcal{A}T}{2} \sum_{\omega_n > 0} \int_{|p_\parallel| < p_F} \frac{d^2 p_\parallel}{(2\pi)^2} \\ & \times \frac{\Delta^2 \omega_n^2 |\beta_1||\beta_2| \nu_1^2 \nu_2^2 \sin\tilde{\chi}}{[\omega_n^2 + \Delta^2(\mathrm{Re}\,\alpha_1)^2][\omega_n^2 + \Delta^2(\mathrm{Re}\,\alpha_2)^2]} \\ & \times \frac{1}{\sinh(2\omega_n d/|v_{Fx}|)}, \end{aligned} \tag{46}$$

which matches with the analogous result derived in Ref. 4 provided we set $\mathrm{Re}\,\alpha_{1,2} = 1$. For $v_F/d \ll T \ll \Delta$, the integral in Eq. (43) is dominated by the contribution of momenta values sufficiently close to $p_\parallel = 0$, and the dependence for the Josephson current on the junction thickness d acquires the standard exponential form

$$I = -\frac{4e\mathcal{A}v_F p_F^2 T^2}{\pi\Delta^2 d} \exp\left(\frac{-2\pi T d}{v_F}\right) \left.\frac{\mathcal{D}_{12}\sin\tilde{\chi}}{|\tilde{\alpha}_1|^2|\tilde{\alpha}_2|^2}\right|_{p_\parallel = 0}. \tag{47}$$

At lower temperatures $T \ll v_F/d \ll \Delta$, Eq. (43) yields the power-law dependence on d:

$$I = -\frac{7\zeta(3)e\mathcal{A}}{4\pi d^3 \Delta^2} \int_{|p_\parallel| < p_F} \frac{d^2 p_\parallel}{(2\pi)^2} \frac{|v_{Fx}|^3 \mathcal{D}_{12} \sin\tilde{\chi}}{|\tilde{\alpha}_1|^2|\tilde{\alpha}_2|^2}, \tag{48}$$

i.e., $I \propto 1/d^3$ at $T \to 0$. In the limit of the small transparencies $\nu_{1,2} \ll 1$ or spin-flip factors $|\beta_1|, |\beta_2| \ll 1$, the term in $Q(\omega)$ proportional to $\cos\tilde{\chi}$ is irrelevant, and the current-phase relation becomes purely sinusoidal,

$$I(\chi) = -I_c \sin(\chi - \chi_0), \tag{49}$$

where the phase shift χ_0 depends on the scattering matrix parameters (45) and, hence, in general can take any value. Provided these values change randomly for different conducting channels, the net Josephson current across the system can be significantly reduced. For symmetric interfaces, the phase shift χ_0 is identically zero and the π-junction behavior is realized.

Note that expression (46) formally diverges in the limit of small d, illustrating the insufficiency of the perturbative (in the transmission) approach for the case of sufficiently short SHS junctions. This divergence is, however, regularized within the nonperturbative approach adopted here. From Eqs. (43) and (44), we observe that for very short junctions $d \ll \xi_0(\nu_1^2 + \nu_2^2)$ (and for $\mathrm{Re}\,\alpha_1 = \mathrm{Re}\,\alpha_2$), the Josephson current scales with the tunnel interface transmissions as

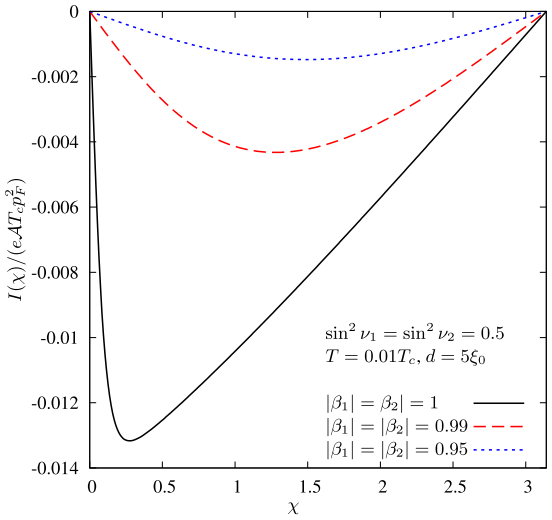

FIG. 2. (Color online) Phase dependence of the Josephson current at low temperatures and different spin-flip factors β. For simplicity, we consider the case of identical interfaces and assume that scattering parameters ν, β, α, and ζ are momentum independent. Parameter α is chosen to be real. The phase coherence length ξ_0 is defined as $\xi_0 = v_F/(2\pi T_c)$.

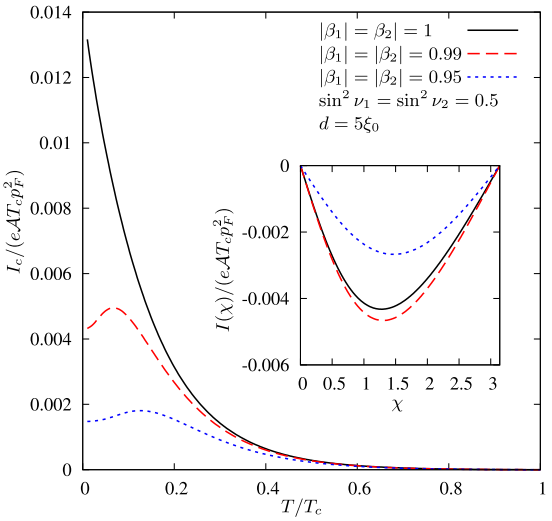

FIG. 3. (Color online) Critical Josephson current I_c as a function of temperature for different spin-flip factors β. The inset shows the current-phase relation for $\beta_1 = \beta_2 = 0.99$ and at temperatures $T/T_c = 0.01$ (solid line), 0.1 (dashed line), 0.2 (dotted line). For simplicity, we consider the case of identical interfaces and assume that scattering parameters ν, β, α, and ζ are momentum independent. Parameter α is chosen to be real.

$$I \propto \frac{\nu_1^2 \nu_2^2}{\nu_1^2 + \nu_2^2}. \tag{50}$$

Obviously, this dependence cannot be derived within a simple perturbative approach in $\nu_{1,2}$.

A detailed analysis of analytical expressions for the current in the limit of high interface transmissions will be postponed to the next section. Here, we only present Figs. 2 and 3 illustrating some key features of our general results (43)–(45). The current-phase relation for sufficiently thick SHS junction is depicted in Fig. 2 at $T = 0.01T_c$ for the case of highly transmitting identical interfaces. We observe that within the interval of Josephson phases χ ranging from zero to π, the current is always negative. Strong deviations from the sinusoidal current-phase relation emerge only provided the spin-flip parameter $|\beta|$ is very close to unity which corresponds to (almost) complete spin-flip scattering at both interfaces. Temperature dependence of the critical Josephson current is shown in Fig. 3 for different values of the spin-flip parameter $|\beta|$. Similarly to Refs. 2 and 4 in a wide parameter range, we find nonmonotonous dependence of the critical current on T with a maximum typically below $0.2T_c$. We also observe that this feature disappears as the spin-flip factor $|\beta|$ approaches unity, i.e., monotonous increase of I_c with decreasing temperature is expected in the limit of complete spin-flip scattering at the HS interfaces.

III. GOING BEYOND QUASICLASSICS

The quasiclassical approach used so far provides an exact solution for the problem in the limit of a large number of conducting channels in our structure. In this case, the quantum mechanical phases, relevant, e.g., for resonance effects, average out.[16] Such averaging is justified in a number of important physical situations, for instance, provided surface roughness of metallic interfaces exceeds the Fermi wavelength. On the other hand, the many-channel limit is not the only one of physical relevance for the systems in question. Modern experimental techniques enable one to study the Josephson current through objects with few conducting channels with controllable change of the scattering phase.[17] This renders a motivation for calculating the Josephson current through such objects. In such cases, the above quasiclassical formalism is, in general, insufficient, and more accurate treatment becomes necessary.[16] In addition, correct description of Andreev states in SHS junctions also requires going beyond the quasiclassical approach employed in Sec. II.

A. General formalism

Below, we will make use of the more general microscopic formalism based of the Gorkov equations. Let us introduce the matrix Matsubara Green's functions[18]

$$G_{ll'}(x_1, x_2, \tau_1 - \tau_2) = -\langle \mathrm{T}_\tau \psi_l(x_1, \tau_1) \bar{\psi}_{l'}(x_2, \tau_2) \rangle, \tag{51}$$

where the indices are numbered as

$$\psi_1 = \psi_\uparrow, \quad \psi_2 = \psi_\downarrow, \quad \psi_3 = \bar{\psi}_\uparrow, \quad \psi_4 = \bar{\psi}_\downarrow. \tag{52}$$

As before, assuming singlet pairing in superconducting electrodes, one can write down the standard Gorkov equations

$$(i\omega_n - [\check{\epsilon}(x_1) + \check{\Delta}(x_1)])\check{G}(x_1, x_2, \omega_n) = \delta(x_1 - x_2), \tag{53}$$

where we performed the Fourier transformation with respect to $\tau_1 - \tau_2$ introducing the Matsubara frequencies ω_n. The matrix operators $\check{\epsilon}, \check{\Delta}$ have the structure

$$\check{\epsilon} = \begin{pmatrix} \epsilon & 0 & 0 & 0 \\ 0 & \epsilon & 0 & 0 \\ 0 & 0 & -\epsilon & 0 \\ 0 & 0 & 0 & -\epsilon \end{pmatrix}, \quad \check{\Delta} = \begin{pmatrix} 0 & 0 & 0 & \Delta \\ 0 & 0 & -\Delta & 0 \\ 0 & -\Delta^* & 0 & 0 \\ \Delta^* & 0 & 0 & 0 \end{pmatrix}, \tag{54}$$

where

$$\epsilon(x_1) = -\frac{1}{2m}\nabla_{x_1}^2 - \frac{p_{Fx}^2}{2m} + V(x_1). \tag{55}$$

Here, $p_{Fx}(v_{Fx})$ is the x component of the Fermi momentum (velocity) for a transmission channel and $V(x)$ stands for the potential energy.

Inside the half metal, it is necessary to account for triplet pairing which amounts to solving the two equations

$$[i\omega_n - \epsilon(x_1)]G_{11}(x_1,x_2,\omega_n) = \delta(x_1 - x_2), \tag{56}$$

$$[i\omega_n + \epsilon(x_1)]G_{31}(x_1,x_2,\omega_n) = 0. \tag{57}$$

The current flowing through the half-metal layer is given by the expression

$$I = \frac{ie}{2m}T\sum_{\omega_n,k}(\nabla_{x_2} - \nabla_{x_1})_{x_2\to x_1}G_{11}(x_1,x_2,\omega_n). \tag{58}$$

Here and below, an additional sum over the channel index k implies summation over all conducting channels of the junction. In the many-channel limit, this summation can be reduced to the integral over the momentum,

$$\sum_k \to \mathcal{A}\int_{|p_\parallel|<p_F}\frac{d^2p_\parallel}{(2\pi)^2}, \tag{59}$$

which we already encountered in Sec. II.

In what follows, we will make use of the standard approximation

$$\nabla_x^2[f(x)e^{\pm ip_{Fx}x}] = [-p_{Fx}^2 f(x) \pm 2ip_{Fx}\partial_x f(x)]e^{\pm ip_{Fx}x}, \tag{60}$$

which is justified for any function $f(x)$ that varies smoothly on atomic distances. We further exactly follow the derivation.[16] Let us fix the argument of the Green's functions x_2 inside the half-metal layer and analyze their dependence on x_1. For instance, we observe that the solution of Eq. (53) decaying deep inside the left superconductor has the form

$$\begin{pmatrix} G_{11} \\ G_{41} \end{pmatrix} = \begin{pmatrix} 1 \\ -ie^{i\chi/2}a \end{pmatrix} e^{-ip_{Fx}x_1}e^{\kappa(x_1+(d/2))}y_1(x_2) + \begin{pmatrix} 1 \\ ie^{i\chi/2}a^{-1} \end{pmatrix} e^{ip_{Fx}x_1}e^{\kappa[x_1+(d/2)]}y_9(x_2). \tag{61}$$

Here, $y_1(x_2), y_9(x_2)$ are arbitrary functions, a is defined below Eq. (12), and $\kappa = \sqrt{\omega_n^2 + |\Delta|^2}/v_{Fx}$. The spatial decay of the functions (G_{21}, G_{31}) is described analogously.

A particular solution of Eq. (56) in the half metal at $\omega_n > 0$ reads

$$G_{11} = -\frac{i}{v_{Fx}}\exp\left[\left(ip_{Fx} - \frac{\omega_n}{v_{Fx}}\right)|x_1 - x_2|\right], \tag{62}$$

$$G_{31} = 0. \tag{63}$$

Further calculation amounts to writing down the general solution in the half-metal layer and to matching it with the decaying solution in the superconducting reservoirs. This matching is made with the help of the scattering matrices that relate outgoing and incoming waves. It is necessary to use two triads: The first one is composed of the functions G_{11}, G_{21} in the superconductor and the function G_{11} in the half metal, while the second one comprises the functions G_{31}, G_{41} of the superconductor and the function G_{31} of the half metal. The second triad accounts for the holelike excitations; hence, it should be described by the transposed scattering matrix.

By matching these two triads at the left and the right interfaces, we arrive at 12 linear equations for the variables $y_1, \ldots, y_{12}$,

$$\begin{pmatrix} y_1 \\ y_2 \\ qy_3 \end{pmatrix} = \hat{S}_1 \begin{pmatrix} y_9 \\ y_{10} \\ z_1 + q^{-1}y_6 \end{pmatrix}, \tag{64}$$

$$\begin{pmatrix} y_4 \\ y_5 \\ qy_6 \end{pmatrix} = \hat{S}_2 \begin{pmatrix} y_{11} \\ y_{12} \\ z_2 + q^{-1}y_3 \end{pmatrix}, \tag{65}$$

$$\begin{pmatrix} ie^{i\chi/2}ay_2 \\ -ie^{i\chi/2}ay_1 \\ q^{-1}y_7 \end{pmatrix} = \hat{S}_1^T \begin{pmatrix} -ie^{i\chi/2}a^{-1}y_{10} \\ ie^{i\chi/2}a^{-1}y_9 \\ qy_8 \end{pmatrix}, \tag{66}$$

$$\begin{pmatrix} ie^{-i\chi/2}ay_5 \\ -ie^{-i\chi/2}ay_4 \\ q^{-1}y_8 \end{pmatrix} = \hat{S}_2^T \begin{pmatrix} -ie^{-i\chi/2}a^{-1}y_{12} \\ ie^{-i\chi/2}a^{-1}y_{11} \\ qy_7 \end{pmatrix}. \tag{67}$$

Here, we keep $\omega_n > 0$, denote $q = \exp(\omega_n d/2v_{Fx})$, and define the scattering matrices $\hat{S}_{1,2}$ as nontrivial 3×3 submatrices in Eq. (31).

The solution of Eqs. (64)–(67) takes the form

$$y_3 = U_1 z_1 + U_2 z_2, \quad y_6 = V_1 z_1 + V_2 z_2. \tag{68}$$

Then, the contribution to the Josephson current defined by the Green's functions with positive Matsubara frequencies reads

$$I_+ = ieT\sum_{\omega_n>0,k} q^{-1}(V_1 - U_2). \tag{69}$$

The contribution to the current from negative Matsubara frequencies I_- is determined analogously. It is straightforward to observe that the total Josephson current acquires the form

$$I = I_+ + I_- = 2\,\mathrm{Re}\, I_+, \tag{70}$$

i.e., it will be sufficient for our purposes to evaluate only the term I_+.

The matrices $S_{1,2}$ relate the amplitudes of incoming and outgoing waves $\exp(\pm ip_{Fx}x)$. So, if the scattering interface is shifted from $x=0$ to $x=x_{1,2}$, these matrices are transformed as

$$\hat{S}_{1,x=x_1} = \hat{\Lambda}_1 \hat{S}_{1,x=0} \hat{\Lambda}_1, \tag{71}$$

$$\hat{\Lambda}_1 = \begin{pmatrix} e^{ip_{Fx}x_1} & 0 & 0 \\ 0 & e^{ip_{Fx}x_1} & 0 \\ 0 & 0 & e^{-ip_{Fx}x_1} \end{pmatrix} \tag{72}$$

and

$$\hat{S}_{2,x=x_2} = \hat{\Lambda}_2 \hat{S}_{2,x=0} \hat{\Lambda}_2, \tag{73}$$

$$\hat{\Lambda}_2 = \begin{pmatrix} e^{-ip_{Fx}x_2} & 0 & 0 \\ 0 & e^{-ip_{Fx}x_2} & 0 \\ 0 & 0 & e^{ip_{Fx}x_2} \end{pmatrix}. \tag{74}$$

B. Supercurrent

Combining the solution of Eqs. (64)–(67) with Eqs. (68) and (69), we find

$$I_+ = ieT \sum_{\omega_n>0,k} \frac{e^{-i\chi}\left(\frac{A(\hat{S}_2,a^2)A^*(\hat{S}_2,a^{-2}) - B(\hat{S}_2,a^2)B(\hat{S}_2,a^{-2})}{\Phi(\hat{S}_2,a^2)\Phi(\hat{S}_2,a^{-2})}\right) - e^{i\chi}\left(\frac{A(\hat{S}_1,a^2)A^*(\hat{S}_1,a^{-2}) - B(\hat{S}_1,a^2)B(\hat{S}_1,a^{-2})}{\Phi(\hat{S}_1,a^2)\Phi(\hat{S}_1,a^{-2})}\right)}{e^{-i\chi}\left(\frac{A(\hat{S}_2,a^2)A^*(\hat{S}_2,a^{-2}) - B(\hat{S}_2,a^2)B(\hat{S}_2,a^{-2})}{\Phi(\hat{S}_2,a^2)\Phi(\hat{S}_2,a^{-2})}\right) + e^{i\chi}\left(\frac{A(\hat{S}_1,a^2)A^*(\hat{S}_1,a^{-2}) - B(\hat{S}_1,a^2)B(\hat{S}_1,a^{-2})}{\Phi(\hat{S}_1,a^2)\Phi(\hat{S}_1,a^{-2})}\right) + \Pi}, \tag{75}$$

where

$$\Pi = \frac{q^4 B(\hat{S}_1,a^2)B(\hat{S}_2,a^2) - A(\hat{S}_1,a^2)A(\hat{S}_2,a^2)}{a^2\Phi(\hat{S}_1,a^2)\Phi(\hat{S}_2,a^2)} + \frac{a^2[q^{-4}B(\hat{S}_1,a^{-2})B(\hat{S}_2,a^{-2}) - A^*(\hat{S}_1,a^{-2})A^*(\hat{S}_2,a^{-2})]}{\Phi(\hat{S}_1,a^{-2})\Phi(\hat{S}_2,a^{-2})} \tag{76}$$

and

$$\begin{aligned} A(\hat{S},a^2) = &- s_{33} + a^2[s_{31}(s_{13}s_{22}^* - s_{23}s_{21}^*) + s_{32}(s_{23}s_{11}^* - s_{13}s_{12}^*) \\ &+ s_{33}(|s_{12}|^2 + |s_{21}|^2 - s_{11}s_{22}^* - s_{22}s_{11}^*)] \\ &+ a^4[s_{12}^*s_{21}^* - s_{11}^*s_{22}^*][s_{31}(s_{23}s_{12} - s_{13}s_{22}) \\ &+ s_{32}(s_{13}s_{21} - s_{23}s_{11}) + s_{33}(s_{11}s_{22} - s_{12}s_{21})], \end{aligned} \tag{77}$$

$$\begin{aligned} B(\hat{S},a^2) = 1 &+ a^2(s_{11}s_{22}^* + s_{22}s_{11}^* - |s_{12}|^2 - |s_{21}|^2) \\ &+ a^4(s_{12}s_{21} - s_{11}s_{22})(s_{12}^*s_{21}^* - s_{11}^*s_{22}^*), \end{aligned} \tag{78}$$

$$\begin{aligned} \Phi(\hat{S},a^2) = s_{13}^*s_{32} - s_{23}^*s_{31} &+ a^2[s_{31}s_{13}^*(s_{22}s_{21}^* - s_{12}s_{22}^*) \\ &+ s_{32}s_{23}^*(s_{21}s_{11}^* - s_{11}s_{12}^*) + s_{31}s_{23}^*(|s_{12}|^2 - s_{22}s_{11}^*) \\ &+ s_{32}s_{13}^*(s_{11}s_{22}^* - |s_{21}|^2)]. \end{aligned} \tag{79}$$

Making use of the parametrization (36) of the scattering matrices, we eventually arrive at the general expression for the Josephson current

$$I = -\frac{8eT}{\Delta^2} \sum_{\omega_n>0,k} \frac{\omega_n^2 \sin\tilde{\chi}}{W - (4\omega_n^2 \cos\tilde{\chi}/\Delta^2)}, \tag{80}$$

where

$$\begin{aligned} W = \frac{1}{2\mathcal{D}_{12}}\{&q^4[(a^{-1}-a)(a^{-1}-a\cos^2\nu_1) + |\tilde{\alpha}_1|^2] \\ &\times[(a^{-1}-a)(a^{-1}-a\cos^2\nu_2) + |\tilde{\alpha}_2|^2] + q^{-4}[(a^{-1}-a) \\ &\times(a^{-1}\cos^2\nu_1 - a) + |\tilde{\alpha}_1|^2][(a^{-1}-a) \\ &\times(a^{-1}\cos^2\nu_2 - a) + |\tilde{\alpha}_2|^2] \\ &- e^{i\varphi}[(a^{-1}-a)^2\cos\nu_1 + \tilde{\alpha}_1^2][(a^{-1}-a)^2\cos\nu_2 + \tilde{\alpha}_2^2] \\ &- e^{-i\varphi}[(a^{-1}-a)^2\cos\nu_1 + \tilde{\alpha}_1^{*2}][(a^{-1}-a)^2\cos\nu_2 + \tilde{\alpha}_2^{*2}]\}. \end{aligned} \tag{81}$$

Here, $\varphi = -2\zeta_1 - 2\zeta_2 + 2p_{Fx}d$ is the quantum mechanical phase corresponding to electron making a cycle between the two interfaces. As we already discussed, in the many-channel limit, it is appropriate to average the result [Eqs. (80) and (81)] over quickly oscillating phase φ. This averaging is accomplished with the aid of the relationship

$$\int_0^{2\pi} \frac{1}{A + Be^{i\varphi} + Ce^{-i\varphi}} \frac{d\varphi}{2\pi} = \frac{1}{\sqrt{A^2 - 4BC}}. \tag{82}$$

It is satisfactory to observe that after such averaging in Eqs. (80) and (81), the general expression for the Josephson current exactly coincides with Eqs. (43)–(45) derived in Sec. II within our quasiclassical analysis.

C. Weak tunneling limit

Let us first analyze the above general results in the limit of low interface transmissions $\nu_1, \nu_2 \ll 1$. In this case, Eq. (81) reduces to

$$W = \frac{1}{\mathcal{D}_{12}\Delta^4}\left\{16\left(\cosh\frac{2\omega_n d}{v_{Fx}} - \cos\varphi\right)[\omega_n^2 + \Delta^2(\mathrm{Re}\,\alpha_1)^2]\right.$$
$$\times[\omega_n^2 + \Delta^2(\mathrm{Re}\,\alpha_2)^2] + 2\omega_n^2\{\nu_1^4[\omega_n^2 + \Delta^2(\mathrm{Re}\,\alpha_2)^2]$$
$$+ \nu_2^4[\omega_n^2 + \Delta^2(\mathrm{Re}\,\alpha_1)^2] + 2\nu_1^2\nu_2^2(\omega_n^2 + \Delta^2)\} + 2\nu_1^4\Delta^2$$
$$\times(\mathrm{Im}\,\alpha_1)^2[\omega_n^2 + \Delta^2(\mathrm{Re}\,\alpha_2)^2] + 2\nu_2^4\Delta^2(\mathrm{Im}\,\alpha_2)^2$$
$$\times[\omega_n^2 + \Delta^2(\mathrm{Re}\,\alpha_1)^2]$$
$$+ 4\nu_1^2\nu_2^2\Delta^4\,\mathrm{Im}\,\alpha_1\,\mathrm{Re}\,\alpha_1\,\mathrm{Im}\,\alpha_2\,\mathrm{Re}\,\alpha_2 - 8\Delta^2\omega_n^2$$
$$\left.(\mathrm{Im}\,\alpha_1\,\mathrm{Re}\,\alpha_1\nu_1^2 + \mathrm{Im}\,\alpha_2\,\mathrm{Re}\,\alpha_2\nu_2^2)\sin\varphi\right\}. \quad (83)$$

The resulting expression for the current for long $d \gg \xi_0$ junctions is given by

$$I = -\frac{eT}{2}\sum_{\omega_n>0,k}\frac{\Delta^2\omega_n^2\mathcal{D}_{12}\sin\tilde{\chi}}{[\omega_n^2 + \Delta^2(\mathrm{Re}\,\alpha_1)^2][\omega_n^2 + \Delta^2(\mathrm{Re}\,\alpha_2)^2]\left(\cosh\frac{2\omega_n d}{v_{Fx}} - \cos\varphi_k\right)}. \quad (84)$$

Here and below, we explicitly indicate the dependence of the scattering phase φ_k on the channel number k. At $T=0$, we obtain

$$I = -\frac{7\zeta(3)e}{4\pi\Delta^2 d^3}\sum_k \frac{v_{Fx}^3\mathcal{D}_{12}\sin\tilde{\chi}}{|\tilde{\alpha}_1|^2|\tilde{\alpha}_2|^2}F(\varphi_k). \quad (85)$$

Comparing this exact result with its quasiclassical analog (48), we observe that in Eq. (85), the contributions of different channels are weighted by the function $F(\varphi_k)$ which reads (see also Fig. 4)

$$F(\varphi) = \frac{2\varphi}{21\zeta(3)\sin\varphi}(\pi - |\varphi|)(2\pi - |\varphi|), \quad (86)$$

where $-\pi \leqslant \varphi \leqslant \pi$. The average of this function over this phase interval equals to unity.

This relatively weak modulation of the Josephson current in our case is in a drastic contrast with the pronounced resonant behavior of the zero-temperature current in conventional SNS junctions, see, e.g., Ref. 16. This difference is formally due to the presence of ω_n^2 in the expression for the Josephson current (80).

Note that although in the limit $d \gg \xi_0$ resonant effects remain insignificant, they gain importance for shorter junctions $d \lesssim \xi_0$, which will be considered below. As before, we stick to the case of weakly transmitting boundaries (small ν, β)

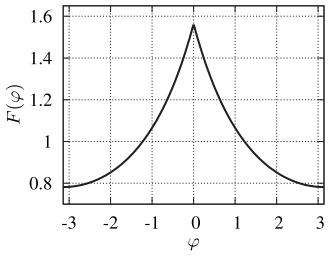

FIG. 4. The function $F(\varphi)$ defined in Eq. (86).

assuming for simplicity $\mathrm{Re}\,\alpha_1 = \mathrm{Re}\,\alpha_2 = 1$. In the many-channel limit, we have for $\xi_0(\nu_1^2 + \nu_2^2) \ll d \lesssim \xi_0$

$$I = \frac{e\Delta}{32\pi^2 Td}\,\mathrm{Im}\,\psi'\left(\frac{1 + i(\Delta/\pi T)}{2}\right)\sum_k \nu_1^2\nu_2^2|\beta_1||\beta_2|v_{Fx}\sin\tilde{\chi}. \quad (87)$$

Here, $\psi'(z) = d^2\ln\Gamma(z)/dz^2$ is the polygamma function. In the limit $T \ll \Delta$, Eq. (87) yields

$$I = -\frac{e}{16\pi d}\sum_k \nu_1^2\nu_2^2|\beta_1||\beta_2|v_{Fx}\sin\tilde{\chi}. \quad (88)$$

We observe that at $T \to 0$, the Josephson current grows with decreasing d as $I \propto 1/d$. This dependence persists down to $d \sim \xi_0(\nu_1^2 + \nu_2^2)$. At even smaller $d \ll \xi_0(\nu_1^2 + \nu_2^2)$, we obtain

$$I = -eT\Delta^2\sum_{\omega_n>0,k}\frac{\omega_n\nu_1^2\nu_2^2|\beta_1||\beta_2|\sin\tilde{\chi}}{(\omega_n^2 + \Delta^2)^{3/2}(\nu_1^2 + \nu_2^2)}, \quad (89)$$

which yields at $T \ll \Delta$

$$I = -\frac{e\Delta}{2\pi}\sum_k \frac{\nu_1^2\nu_2^2|\beta_1||\beta_2|\sin\tilde{\chi}}{\nu_1^2 + \nu_2^2}. \quad (90)$$

The above results correspond to effective averaging of the φ-dependent Josephson current. Let us now see how these results get modified if the resonance condition $\cos\varphi = 1$ holds for some of the conducting channels. In this case, we have

$$I = -\frac{e}{32d^2\Delta}\frac{\sinh\frac{\Delta}{T} - \frac{\Delta}{T}}{1 + \cosh\frac{\Delta}{T}}\sum_k{}' \nu_1^2\nu_2^2|\beta_1||\beta_2|v_{Fx}^2\sin\tilde{\chi}, \quad (91)$$

for $d \gg \xi_0(\nu_1^2 + \nu_2^2)$, and

$$I = -e\Delta \tanh\frac{\Delta}{2T}\sum_k{}' \frac{\nu_1^2\nu_2^2|\beta_1||\beta_2|\sin\tilde{\chi}}{(\nu_1^2+\nu_2^2)^2}, \tag{92}$$

in the limit $d \ll \xi_0(\nu_1^2+\nu_2^2)$. Here, the sum Σ_k' runs over the resonant channels only.

The resonant currents (91) and (92) turn out to be much larger than the corresponding phase-averaged contributions (87) and (89). Correspondingly, the resonances are quite narrow: $\delta\varphi \sim d/\xi_0$ and $\delta\varphi \sim \nu_1^2+\nu_2^2$ for longer and shorter junctions. The off-resonant currents are smaller in the measure of d^2/ξ_0^2 and $(\nu_1^2+\nu_2^2)^2$, respectively.

D. High transmission limit

For completeness, let us analyze the case of fully transmitting interfaces, i.e., $\sin^2\nu_1 = \sin^2\nu_2 = 1$. For short $d \ll \xi_0$ junction, the Josephson current is defined by Eq. (80) with

$$W = \frac{2}{|\beta_1||\beta_2|} \times\left(|\alpha_1|^2|\alpha_2|^2\sin^2\frac{\varphi}{2} + 4\frac{\omega_n^4}{\Delta^4} + (2+|\alpha_1|^2+|\alpha_2|^2)\frac{\omega_n^2}{\Delta^2}\right). \tag{93}$$

Here, the initial phase φ is shifted by $2\arg\alpha_1 + 2\arg\alpha_2$. In particular, at low temperatures $T \ll \Delta$ and for small $\beta_{1,2}$, we have

$$I = -\frac{e\Delta}{4}\sum_k \frac{|\beta_1||\beta_2|\sin\tilde{\chi}}{\sqrt{1+\left|\sin\frac{\varphi_k}{2}\right|}}. \tag{94}$$

In the opposite long junction limit $d \gg \xi_0$ and at $T \ll \Delta$, the Josephson current is again given by Eq. (80), where one should substitute

$$W = \frac{1}{|\beta_1||\beta_2|}\left[\left(\cosh\frac{2\omega_n d}{v_{Fx}} - \cos\varphi\right)|\alpha_1|^2|\alpha_2|^2 + \frac{2\omega_n^2}{\Delta^2}(2+|\alpha_1^2| + |\alpha_2|^2)\cosh\frac{2\omega_n d}{v_{Fx}} + 2\frac{\omega_n}{\Delta}\sinh\frac{2\omega_n d}{v_{Fx}}(|\alpha_1|^2+|\alpha_2|^2)\right]. \tag{95}$$

For $|\alpha_{1,2}| \sim 1$, we again recover Eq. (85), in which we should replace $\tilde{\alpha}_{1,2}$ by $\alpha_{1,2}$.

Of special interest is the case of identical interfaces with $|\beta_{1,2}| = 1$ which corresponds to equal probabilities for spin-up and spin-down electrons to penetrate into the half metal.

In this case, Eqs. (93) and (95) yield

$$I = -\frac{e\Delta}{2}\mathcal{N}\,\mathrm{sgn}\,\chi\cos\frac{\chi}{2} \tag{96}$$

for $d \ll \xi_0$ and

$$I = \frac{e}{2\pi d}(\chi - \pi\,\mathrm{sgn}\,\chi)\sum_k v_{Fx} \tag{97}$$

for $d \gg \xi_0$. Here, the Josephson phase difference is restricted within the interval $-\pi \leqslant \chi \leqslant \pi$, and the total number of conducting channels in our SHS junction is denoted by $\mathcal{N}$. One easily recognizes that Eqs. (96) and (97) are nothing but the π-shifted Kulik-Omel'yanchuk[19] and Ishii-Kulik[20] current-phase relations, respectively, for short and long SNS junctions. It is also interesting to observe that for $\mathcal{N}=2$ (i.e., in the single channel limit with two spin directions), Eq. (97) coincides with the result for the Josephson current in long SNS junctions embedded in a superconducting ring with odd number of electrons.[21] It also follows from Eq. (95) that the current-phase relation (97) for long junctions $d \gg \xi_0$ sets in only in the narrow parameter region $|\alpha_1|^2|\alpha_2|^2 \lesssim \xi_0^2/d^2$. Correspondingly, the dependence of the Josephson current on the H-layer thickness changes from $I \propto 1/d^3$ to $I \propto 1/d$.

E. Andreev states

The expressions for the Green's functions and for the Josephson current derived above enable us to obtain the spectrum of subgap Andreev bound states inside the half metal. Substituting $\omega_n \to -iE$, we easily find the poles of the Green's function which provide the required spectrum. For junctions $d \gg \xi_0$ with low transparency (small β, ν), it is governed by the equation

$$\cos\left(\frac{2Ed}{v_{Fx}}\right) - \cos\varphi + \frac{E^2\mathcal{D}_{12}\cos\tilde{\chi}}{4\Delta^2(\mathrm{Re}\,\alpha_1)^2(\mathrm{Re}\,\alpha_2)^2} = 0. \tag{98}$$

Here, we assume that $E \ll \Delta$ and $\mathrm{Re}\,\alpha_1 \sim \mathrm{Re}\,\alpha_2 \sim 1$. Though the third term in this equation is much smaller than the other two, it is important since it determines the dependence of the spectrum on the Josephson phase χ. Note that the above equation remains valid for all values of φ except for an immediate vicinity of the resonance $\cos\varphi = 1$ where the full expression for W has to be taken into account. In the latter limit, the result becomes rather cumbersome and is omitted here.

It is instructive to compare the above expression with that for Andreev bound states in conventional SNS junctions in the limit of low transmissions $D_{1,2}$ of NS interfaces, see, e.g., Ref. 16. For long SNS junctions $d \gg \xi_0$, we have

$$\cos\left(\frac{2Ed}{v_{Fx}}\right) - \cos\varphi + \frac{D_1D_2}{4}\cos\chi = 0. \tag{99}$$

As before, the parameter φ is defined as $\varphi = \varphi_0 + 2p_{Fx}d$. In the limit $D_{1,2} = 0$, this equation describes particle- and holelike excitations inside the normal layer with impenetrable boundaries. At small but nonzero $D_{1,2}$, these states get modified due to the superconducting proximity effect. We observe that in the presence of triplet pairing states inside our SHS junction, Eq. (98) has essentially the same structure as Eq. (99) describing singlet pairing states except for an additional small factor E^2/Δ^2 entering the χ-dependent term in the triplet case.

In the opposite limit of short junctions $d \ll \xi_0$, the spectrum of Andreev levels can be found analogously. For SHS junctions we obtain

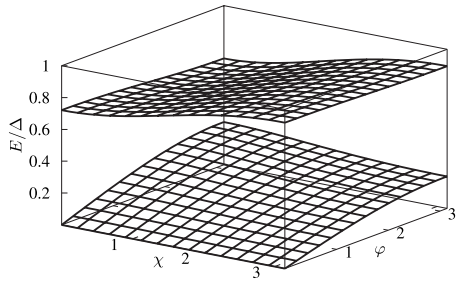

FIG. 5. The higher and lower Andreev levels in short SHS junctions with highly transparent interfaces for $|\beta_1|=|\beta_2|=0.8$.

$$(1-\cos\varphi)\left((\mathrm{Re}\,\alpha_1)^2-\frac{E^2}{\Delta^2}\right)\left((\mathrm{Re}\,\alpha_2)^2-\frac{E^2}{\Delta^2}\right)+\frac{E^2}{4\Delta^2}\mathcal{D}_{12}\cos\tilde{\chi}=0. \tag{100}$$

In the case $\mathrm{Re}\,\alpha_{1,2}\approx 1$, this result describes excitations that are slightly below the gap.

For comparison, we also recall the well known expression which defines the spectrum of Andreev levels for short ($d \ll \xi_0$) conventional SNS junctions:

$$\cos\varphi\left(\frac{E^2}{\Delta^2}-1\right)\left(1-\frac{(D_1+D_2)^2}{8}\right)+1-\frac{E^2}{\Delta^2}-\frac{D_1D_2}{4}(1-\cos\chi)=0. \tag{101}$$

Similarly to Eq. (100), this equation describes the states with energies slightly below the gap. We would also like to point out that Andreev states in SNS junctions are doubly degenerate. This degeneracy, is in general, lifted in the case of triplet pairing states in SHS junctions, see also Ref. 22.

Turning to the limit of highly transparent interfaces, in the limit of long ($d \gg \xi_0$) SHS junctions for $|\alpha_{1,2}|\sim 1$, we again arrive at Eq. (98) where one should only replace $(\mathrm{Re}\,\alpha_{1,2})^2$ by $|\alpha_{1,2}|^2/4$. In the opposite short junction limit $d \ll \xi_0$, we obtain the following equation, which is valid for arbitrary relationship between parameters α and β:

$$4\frac{E^4}{\Delta^4}-(2-2|\beta_1||\beta_2|\cos\tilde{\chi}+|\alpha_1|^2+|\alpha_2|^2)\frac{E^2}{\Delta^2}+|\alpha_1|^2|\alpha_2|^2\sin^2\frac{\varphi}{2}=0. \tag{102}$$

For positive energies $0 \leqslant E \leqslant \Delta$, it has two solutions which are depicted in Figs. 5 and 6 for the case of fully transparent SH interfaces $\sin^2\nu_{1,2}=1$.

We observe that for $|\beta_{1,2}|\approx 1$ (see Fig. 5), the position of Andreev levels significantly depends on the Josephson phase $\tilde{\chi}$, whereas the φ dependence remains not very pronounced. In the limit $|\beta_{1,2}|=1$, the energy of the lower Andreev level reduces to zero, while the energy for the upper one is determined by a simple formula

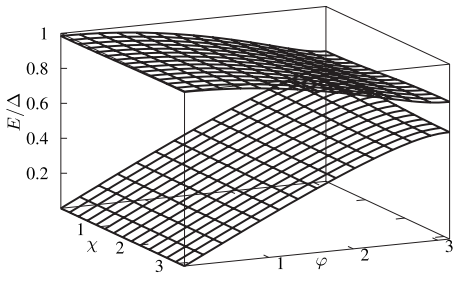

FIG. 6. The same as in Fig. 5 for $|\beta_1|=|\beta_2|=0.2$.

$$E=\Delta|\sin(\tilde{\chi}/2)|. \tag{103}$$

Note that this dependence is just the π-shifted one as compared to the well known dependence $E=\Delta|\cos(\chi/2)|$ for the doubly degenerate Andreev level in short SNS junctions.

In the limit of small spin-flip factors $|\beta_{1,2}|$, the behavior of Andreev levels changes considerably, as illustrated in Fig. 6. In this case, the dependence of the level positions on the Josephson phase $\tilde{\chi}$ is much weaker, whereas their φ dependence becomes more significant.

Clearly, Andreev levels with negative energies $-\Delta \leqslant E \leqslant 0$ are fully symmetric with respect to the Fermi level and, hence, show exactly the same features, as illustrated by Fig. 7. We again observe that the $\tilde{\chi}$ dependence of all four Andreev states is rather pronounced for large values of the spin-flip parameter $|\beta|$ and it almost disappears for small values of $|\beta|$.

IV. SUMMARY

In this paper, we have developed a detailed microscopic theory describing dc Josephson effect and Andreev bound states in superconducting junctions with a half metal. The possibility to pass supercurrent through such SHS junctions

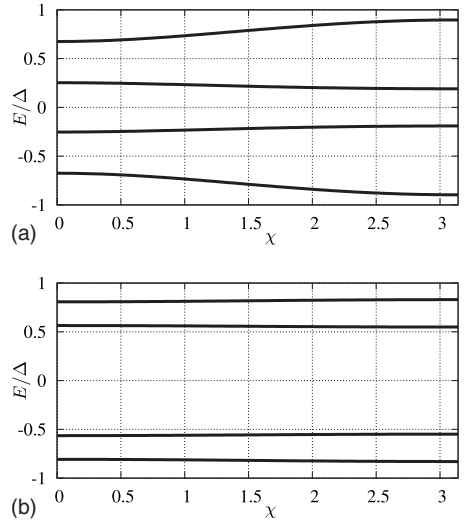

FIG. 7. The structure of Andreev bound states in short SHS junctions with highly transparent interfaces for $|\beta_1|=|\beta_2|=0.8$ (upper figure) and $|\beta_1|=|\beta_2|=0.2$ (lower figure) at $\varphi=2.5$.

is provided by spin-flip scattering at both SH interfaces. As a result, superconducting correlations penetrate into the half metal in the form of triplet pairing states which can carry nonvanishing supercurrent across the system. Our general results for the Josephson current, Eqs. (43) and (80), provide a detailed description of the effect for sufficiently clean metals and at arbitrary transmissions $\sin^2 \nu_{1,2}$ of both interfaces as well as at arbitrary values of the spin-flip parameters $\beta_{1,2}$. In the tunneling limit, our results reduce to those of Ref. 4 derived perturbatively in the interface transmissions. Our approach allows to go beyond the perturbation theory in $\nu_{1,2}$ and to fully account for all orders in interface transmissions. This nonperturbative analysis is unavoidable not only at high transmissions but also in the tunneling limit in the case of sufficiently short junctions in order to eliminate an intrinsic divergence of perturbative results at small d. At $T=0$, the Josephson current depends on the H-layer thickness as $I \propto 1/d^3$ for $d \gg \xi_0$. This dependence then crosses over to $I \propto 1/d$ for $\xi_0(\nu_1^2+\nu_2^2) \ll d \ll \xi_0$ [see Eq. (87)]. Finally, the current becomes d independent at $d \ll \xi_0(\nu_1^2+\nu_2^2)$ [see Eq. (89)]. This saturation of the d dependence of the Josephson current is accompanied by the change of its scaling with ν from $I \propto \nu^4$ to $I \propto \nu^2$. For short junctions $d \ll \xi_0$ with few conducting channels, resonant effects play an important role causing substantial enhancement of the Josephson current, see Eqs. (91) and (92).

Our analysis demonstrates that the behavior of both the Josephson current and Andreev bound states in SHS structures crucially depends on the spin-flip parameters $\beta_{1,2}$. Similarly to Refs. 2 and 4, we observe that for incomplete spin-flip scattering, the temperature dependence of the critical Josephson current is nonmonotonous with a maximum at nonzero T, see Fig. 3. However, this feature disappears completely for $\beta_{1,2} \to 1$ and the Josephson current monotonously increases with decreasing T in this limit. Another striking feature of our results is that SHS junctions are characterized by the sinusoidal current-phase relation at any temperature, and interface transmissions provided the spin-flip parameters $\beta_{1,2}$ are not very close to unity. Substantial deviations of the current-phase relation occur only provided (i) interface transmissions remain high, (ii) temperature remains low, and (iii) the spin-flip parameters $\beta_{1,2}$ are very close to 1, see Fig. 2.

It also follows from our analysis that for symmetric SHS junctions (meaning that electron scattering at both interfaces is described by identical S matrices), the π-junction state is usually realized. However, in a general case where the Josephson current in SHS junctions does not necessarily show the π-junction behavior, the current-phase relation is characterized by an arbitrary phase shift, see Eq. (45). It is also interesting to observe that in the case of fully transmitting interfaces, at $T=0$ and for $|\beta_{1,2}|=1$, our results reduce to very simple dependencies, Eqs. (96) and (97), which are essentially the π-shifted Kulik-Omelyanchuk[19] and Ishii-Kulik[20] current-phase relations, respectively, for short and long SNS junctions.

We believe that our predictions can help identify triplet pairing current states in future experiments with SHS structures.

ACKNOWLEDGMENTS

We acknowledge useful discussions with M. Eschrig. This work was supported in part by RFBR Grant No. 06-02-17459.

[1] R. S. Keizer, S. T. B. Goennenwein, T. M. Klapwijk, G. Miao, G. Xiao, and A. Gupta, Nature (London) **439**, 825 (2006).
[2] M. Eschrig, J. Kopu, J. C. Cuevas, and G. Schön, Phys. Rev. Lett. **90**, 137003 (2003).
[3] Y. Asano, Y. Tanaka, and A. A. Golubov, Phys. Rev. Lett. **98**, 107002 (2007); Y. Asano, Y. Sawa, Y. Tanaka, and A. A. Golubov, Phys. Rev. B **76**, 224525 (2007).
[4] M. Eschrig, T. Löfwander, T. Champel, J. C. Cuevas, J. Kopu, and G. Schön, J. Low Temp. Phys. **147**, 457 (2007).
[5] M. Eschrig and T. Löfwander, Nat. Phys. **4**, 138 (2008).
[6] F. S. Bergeret, A. F. Volkov, and K. B. Efetov, Rev. Mod. Phys. **77**, 1321 (2005).
[7] A. F. Volkov, F. S. Bergeret, and K. B. Efetov, Phys. Rev. Lett. **90**, 117006 (2003).
[8] G. Eilenberger, Z. Phys. **214**, 195 (1968).
[9] For a review see, e.g., W. Belzig, F. K. Wilhelm, C. Bruder, G. Schön, and A. D. Zaikin, Superlattices Microstruct. **25**, 1251 (1999).
[10] M. Eschrig, Phys. Rev. B **61**, 9061 (2000).
[11] A. V. Zaitsev, Sov. Phys. JETP **59**, 1015 (1984).
[12] A. Millis, D. Rainer, and J. A. Sauls, Phys. Rev. B **38**, 4504 (1988).
[13] M. S. Kalenkov and A. D. Zaikin, Phys. Rev. B **75**, 172503 (2007); **76**, 224506 (2007); Physica E (Amsterdam) **40**, 147 (2007); Pis'ma v ZheTF **87**, 166 (2008).
[14] M. Fogelström, Phys. Rev. B **62**, 11812 (2000).
[15] E. Zhao, T. Löfwander, and J. A. Sauls, Phys. Rev. B **70**, 134510 (2004).
[16] A. V. Galaktionov and A. D. Zaikin, Phys. Rev. B **65**, 184507 (2002).
[17] P. Jarillo-Herrero, J. A. van Dam, and L. P. Kouwenhoven, Nature (London) **439**, 953 (2006).
[18] A. A. Abrikosov, L. P. Gorkov, and I. Ye. Dzyaloshinski, *Quantum Field Theoretical Methods in Statistical Physics*, 2nd ed. (Pergamon, Oxford, 1965).
[19] I. O. Kulik and A. N. Omel'yanchuk, Sov. J. Low Temp. Phys. **4**, 142 (1978).
[20] C. Ishii, Prog. Theor. Phys. **44**, 1525 (1970); I. O. Kulik, Sov. Phys. JETP **30**, 944 (1970).
[21] S. V. Sharov and A. D. Zaikin, Phys. Rev. B **71**, 014518 (2005); Physica E (Amsterdam) **29**, 360 (2005).
[22] M. Eschrig, J. Kopu, A. Konstandin, J. C. Cuevas, M. Fogelström, and G. Schön, Adv. Solid State Phys. **44**, 533 (2004).